

Sub-Band Analysis of NLoS Indoor Channel Responses

Dana Porrat and Yuval Serfaty
The Hebrew University of Jerusalem
Jerusalem, Israel 91904
dporrat@cs.huji.ac.il, yuval.ser@gmail.com

Abstract—Key factors of indoor NLoS radio channels are examined, namely the number of channel taps, the mean delay, the RMS delay spread and the channel gain. We analyze wide-band (2-11 GHz) results in bands of 528 MHz and examine the mean behavior of the parameters vs. transmitter-receiver separation, with separations of up to 30 meters, as well as the parameters' correlation across sub-carrier frequency. The mean dependence of the parameters on terminal separation is approximated by a simple linear fit. The measurements were taken in three office buildings in the Givat Ram campus of the Hebrew University with the terminals in the same and in adjacent floors.¹

I. INTRODUCTION

The channel modeling aspects of wideband communications have drawn a lot of interest since the un-licensing of ultra wideband (UWB) systems in the United States in 2002, and numerous measurement campaigns were conducted in industry and academia [1], [2], [3], [4], [5], [6], [7], [8], [9]. The IEEE standardization effort of UWB systems did not yield an agreement of the best technology for communications, but had a significant contribution in the channel model it produced [10].

The Multiband OFDM Alliance (MBOA), established to formulate an industry-based standard for UWB communications, suggested dividing the 3-10 GHz spectrum to 14 sub-bands. Motivated by the sub-band approach, this paper presents measurement results of the mean (excess) delay, RMS delay spread and the significant number of channel taps apparent over individual sub-bands. We also analyze channel gain (path loss) vs. terminal separation and frequency. We characterize the dependence of the measured parameters on the transmitter-receiver separation, in office building settings with no line of sight. Our investigation of the dependence of the parameters other than the channel gain on sub-carrier frequency did not yield a significant trend of the parameter values vs. carrier frequency.

This paper uses the MBOA defined sub-bands with carrier frequencies between 3.432 GHz and 10.296 GHz and 528 MHz bandwidth, with two adjacent sub-bands centered at 2.376 GHz and 2.904 GHz. Our measurement included terminal separations of 5 - 30 meters.

Our measurements include a larger ranges of terminal separation distances and a wider band than presented by most

of the publicly available literature on channel sounding. We briefly overview recent relevant results: [11] presents LoS and NLoS measurements along a single corridor and analyzes the channel gain, the RMS delay spread and the exponential decay rate of the response. This analysis is focused on the carrier frequency dependence of the parameters in 528 MHz bands. [3] show the delay spread and channel gain for two NLoS measurements in the 1-11 GHz band with terminal separation of up to 10 meters. [2] analyze five NLoS measurements, each with numerous receiver positions along a 2.35 meter rail. They show channel gain vs. sub-band carrier frequency for NLoS settings, using 100 MHz bands, and calculate the delay spread and the number of paths. [9] present two NLoS measurements, and show delay spread and channel gain (Table 1 there) for 500 MHz bands between 2 GHz and 6 GHz. [4] show mean delay, RMS delay spread and the exponential decay factor vs. terminal separation with distances of up to 10 m. They calculate the mean and the variance of each of the three parameters over an unspecified number of measurements. [6] present channel gain vs. terminal separation along a corridor for NLoS measurements in the 1-11 GHz range.

II. MEASUREMENTS

A. Equipment

The measurement setup was based on an Agilent N5230 network analyzer, connected to two omni-directional antennas (Electro-Metrics EM-6865) with suitable amplifiers. The antennas were positioned at the same height above the floor. Measurements were swept over the 2-11 GHz range, with a frequency resolution of 1.06 MHz (16001 point per sweep). The antennas were placed on carts that were moved to different locations for different measurements, and were immobile during each measurement. A computer controlled the location of the receiving antenna over a rail, as well as the parameters of the network analyzer and the data collection, that was lengthy since we tried to achieve a high signal to noise ratio over a wide band and used a 50 Hz IF bandwidth. The equipment is further described in the laboratory website at <http://www.cs.huji.ac.il/~dporrat/lab.html>.

B. The Measurement Environment

The 42 measurements analyzed in this paper were collected during 2006–2008 in three buildings in the Givat Ram Campus of the Hebrew University in Jerusalem, namely the Ross

¹This research was supported by the Israel Science Foundation (Grant No. 249/06), and by the Israeli Consortium of Short Range Communications

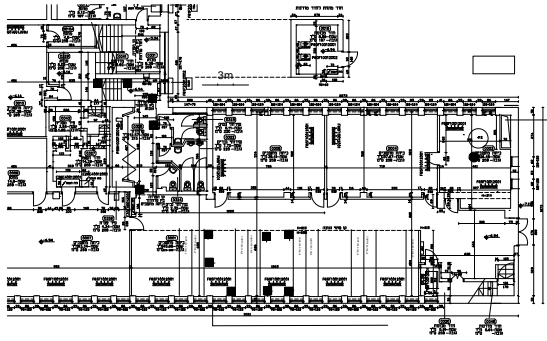


Fig. 1. The Ross Building, Floor -2. The receiver was located in the room on the top right of the figure for all the Ross measurements (marked by a circle). Transmitter locations are indicated by rectangles.

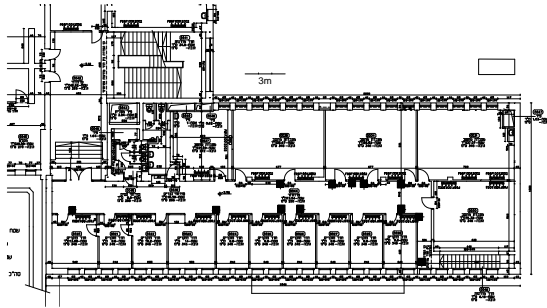


Fig. 2. The Ross Building, Floor -1. The receiver was located one floor below (see Figure 1). Transmitter locations are indicated by rectangles.

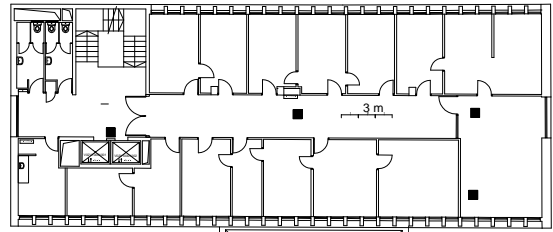


Fig. 4. The Sherman Building, 4th floor. The receiver was located in the 5th floor (Figure 3) and transmitter locations are indicated by rectangles.

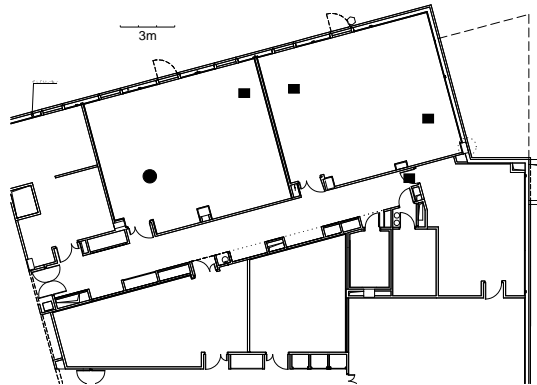


Fig. 5. The New Laboratory Building with the receiver location indicated by a circle and transmitter locations indicated by rectangles.

Building (Figures 1, 2), the Sherman Building (Figures 3, 4 and the New Laboratories Building (Figure 5). The first two are conventional office building built during the 1960s, of reinforced concrete and concrete blocks, and the last was built during the 2000s, with plasterboard interior walls. The transmitter and receiver were located in the same floor and in adjacent floors. Most of the measurements were taken during nights in order to minimize the effect of movement of people.

III. METHODS

The results presented below are based on impulse responses averaged over 10 cm of receiver antenna locations (20 to 26 points) per transmitter antenna location, out of the many measurements taken with different receiver positions along a rail. The averaging effectively took place over very similar

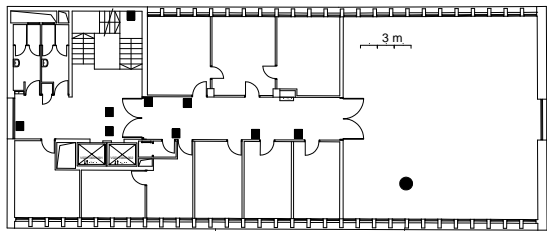


Fig. 3. The Sherman Building, 5th floor. The receiver was located in the big room on the right of the figure for all the Sherman measurements. Transmitter locations are indicated by rectangles.

responses, and had little effect on the results. Our impulse response data were obtained by transforming the sampled frequency domain measurements. After normalization by the frequency dependent antenna gain we used a Raised Cosine Window on the frequency dependent measurements in order to lower the temporal lobes that accompany strong paths. These ‘side-lobes’ are a computational effect resulting from the finite bandwidth. For the full-band analysis we used a window with 1 GHz rising/falling bandwidth, with -3 dB at 2 and 11 GHz. For the sub-band analysis we used a window with 50 MHz rising/falling bandwidth, with a -3 dB bandwidth of 528 MHz. For the full-band analysis we zero pad the measurements below the measured band and use a symmetric conjugate extension in order to ensure a real impulse response [2]. The effective band of the measurements is 2-11 GHz and the temporal resolution of the full-band data is $\Delta t_{FB} = 111$ psec. Removal of the azimuthal direction dependence of the antenna response is not feasible in NLoS measurements, and compensation of elevation dependence as in [11] was not necessary as our antennas were positioned at equal heights.

We analyze the channel gain in Section IV-A vs. terminal separation and frequency. After smoothing and transforming the data to the time domain, we trim it (i.e. limit the time domain of interest) at a level that is -25 dB below the maximum, in order to avoid processing noise. The trimming is done by determining the minimal and maximal delay values where the response crosses the threshold, and considering the response only between these two delay values. The sensitivity

of RMS delay spread calculated from measurements to the threshold level is discussed in [12]. Our threshold of -25 dB agrees with the SNR available in all our measurements.

The next processing step involves normalizing the (squared and trimmed) impulse response into a power delay profile, i.e. a positive function with a unit integral. The normalized power delay profile is marked $\{p_n\}$ where n indicates the temporal (delay) index.

We consider two time spread measures: The mean (excess) delay in Section IV-B and the RMS delay spread in Section IV-C. The mean delay τ_m and the RMS delay spread τ_{RMS} are calculated by a discrete (sum) approximation of the standard definition:

$$\tau_m = \sum_{n=1}^{\infty} n p_n \Delta t \quad \tau_{\text{RMS}} = \sqrt{\sum_{n=1}^{\infty} (n - \tau_m)^2 p_n \Delta t}$$

We calculate in Section IV-D the number of taps that are within 10 dB from the peak of the power delay profile.

To clarify the processing we consider the parameter par that stands for the mean delay, the RMS delay spread and the number of significant taps in different parts of the text. We start with 672 values of the parameter $par(d, f)$, calculated from 42 terminal locations and 16 sub-bands per location. Averaging over the sub-carrier frequency yields a linear approximation of the form $par(d) \approx \text{const } d + \text{const}$, where d stands for terminal (antenna) separation in meters. Linear fits of this type are presented in Figures 7, 9 and 11 for the different parameters we consider, along with the related mean square error (MSE) values.

Analysis then proceeds to the correlation coefficient of each parameter across sub-bands. To calculate the correlation coefficient we subtract the separation dependent linear trend from the parameter values, and use the result to calculate the variance and the correlation between the parameter values across different sub-bands. The correlation coefficient of the parameter measured on sub-bands with center frequencies f and $f + \Delta f$ is given in (1):

$$\begin{aligned} \text{corr}(f, \Delta f) &= \frac{1}{42} \sum_{d_i} [par(d_i, f) - par(d_i)] \\ &\quad [par(d_i, f + \Delta f) - par(d_i)] \\ \text{var}(f) &= \frac{1}{42} \sum_{d_i} [par(d_i, f) - par(d_i)]^2 \\ \rho(f, \Delta f) &= \frac{\text{corr}(f, \Delta f)}{\sqrt{\text{var}(f)\text{var}(f + \Delta f)}} \end{aligned} \quad (1)$$

where the nominator is the covariance and the denominator is the variance, Δf is a multiple of 528 MHz and f is a center frequency of a suitable sub-band. Averaging over the frequency f in order to calculate the correlation coefficient vs. frequency separation gives

$$\rho_{par}(\Delta f) = \frac{1}{\# \text{ of suitable center frequencies}} \sum_f \rho_{par}(f, \Delta f)$$

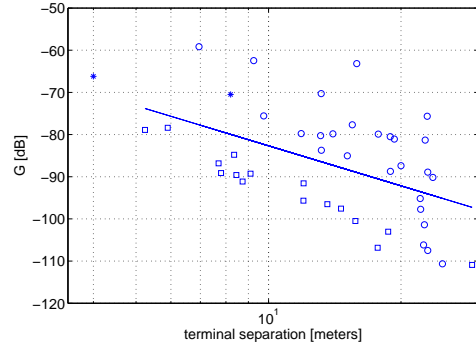


Fig. 6. The channel gain vs. terminal separation in a log-log graph. The circles (\circ) indicate measurements with the terminals in the same floor and the squares (\square) show results with the terminals in adjacent floors. The linear fit is given by $G^2(d) \sim d[\text{m}]^{-3.2}$. The asterisks ($*$) indicate results from [9]: $L=-66.2$ dB for $d=4$ m and $L=-70.5$ dB for $d=8.2$ m (Table 1 and Figure 4), these two measurements may be close to LoS.

The correlation coefficient vs. sub-band carrier separation is plotted in Figures 8, 10 and 12 along with the best (minimum MSE) linear fit.

IV. RESULTS

A. Channel Gain

We plot the channel gain (path loss) in a logarithmic (dB) scale vs. log terminal separation. A straight line with slope $-n$ in this representation indicates a power connection between the terminal separation d and the received power G : $G \sim d^{-n}$. This type of connection is the common model for mean path loss dependence on terminal separation. The parameter n is often termed ‘path loss exponent’.

The linear fit of Figure 6 gives a path loss exponent of 3.2. Plotting the channel gain vs. terminal separation results in a smaller variability (i.e. smaller MSE around the linear fit) if the measurements are separated according to the location of the terminals in the same or in adjacent floors.

[11] show exponents of 1.62 for LoS and 3.22 of NLoS, their tight linear fit probably has to do with the environment of their measurements, that consisted of a single corridor. [6] show in their Figure 9 path loss exponent results of 1.96 for NLoS. [2] find path loss exponents that range from 3.0 at a carrier frequency of 3.15 GHz, an exponent of 2.9 at a carrier frequency of 5.6 GHz and 4.1 at 7.95 GHz, with a bandwidth of 100 MHz.

After fitting the gain vs. frequency plot to a linear approximation and averaging over our measurements, we found that the average linear frequency dependence of the gain is given by -3.8 dB/GHz. We note that [3] find a slope of about 15.3 dB/GHz for a single NLoS measurement (calculated from Figure 12 there). [9] find slopes of 50 dB/GHz and 60 dB/GHz for NLoS measurements with terminal separations of 4 m and 8.2 m, with a single wall (of an unspecified type) separating the terminals, over the band 2-6 GHz. Their results are each based on two measurements.

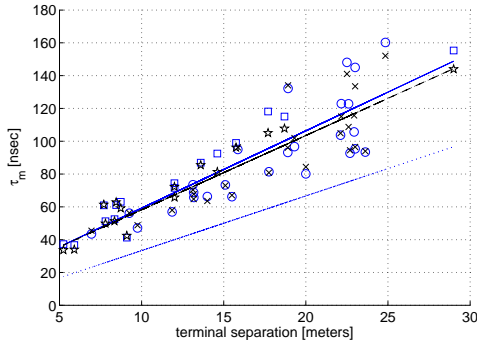


Fig. 7. Mean (excess) delay vs. terminal separation. The circles (o) indicate sub-band results averaged over the 16 sub-bands with antennas located in the same floor, and the squares (□) show results with the terminals in adjacent floors. The full line (—) is a linear fit of all the averaged sub-band results. The Xs (x) show full-band results with the terminals located in the same floor and the stars (*) show full band results with the terminals in adjacent floors. The dashed line (--) is a linear fit of all the full band results, and the dotted line shows free space delays calculated from the terminal separation, the free space slope equals $1/c = 3.33$ nsec/m. The linear fit of the sub-band data (full line) is given by $\tau_m^{SB}(d)[\text{nsec}] = 4.7 d[\text{m}] + 12$ and the full band best fit is $\tau_m^{FB}(d)[\text{nsec}] = 4.5 d[\text{m}] + 13$. The corresponding MSE are 15.3 nsec for the sub-band data and 13.0 nsec for the full-band data.

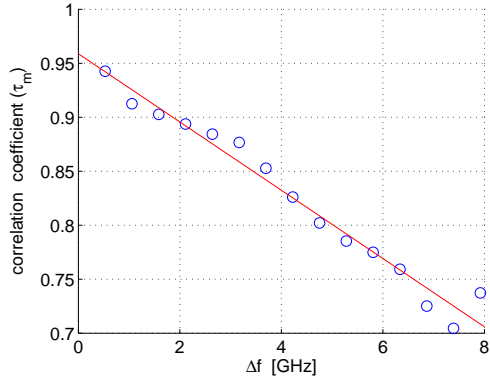


Fig. 8. Mean delay correlation across sub-bands, the linear fit is given by $R_{\tau_m} = -0.032\Delta f[\text{GHz}] + 0.96$.

B. Mean Delay

Figure 7 shows the mean delay vs. terminal separation. The per-band mean delay is similar to the delay measured over the entire (9 GHz) band, contrary to results from [2] that show a higher per-band mean delay. The mean delay values calculated over adjacent sub-bands are correlated as seen in Figure 8.

C. RMS Delay Spread

Figure 9 shows the averaged sub-band RMS delay spread as well as the full band RMS delay spread, vs. terminal separation. The RMS delay spread values calculated over adjacent sub-bands are correlated as seen in Figure 10.

[2] present RMS delay spread values averaged over measurements with unspecified terminal separations that appear between 6 m and 13 m from the floor plan in their Figure 2. They find RMS delay spreads of 18 nsec, 17 nsec and 16 nsec

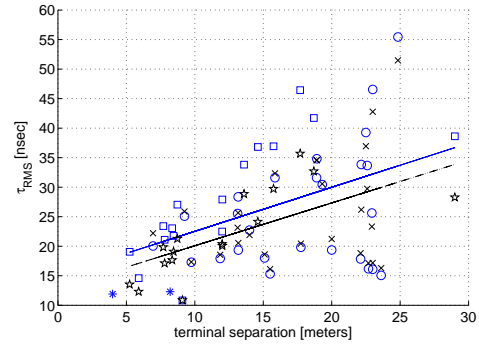


Fig. 9. RMS delay spread vs. terminal separation, see the legend in the caption of Figure 7. The linear fit of the sub-band data (full line) is given by $\tau_{\text{RMS}}^{SB}(d)[\text{nsec}] = 0.75 d[\text{m}] + 15$ (with $\text{MSE}=8.9$ nsec), and the full band data fit is $\tau_{\text{RMS}}^{FB}(d)[\text{nsec}] = 0.73 d[\text{m}] + 13$ (with $\text{MSE}=7.1$ nsec). The asterisks (*) indicate results from [9] (Table 1 there): $\tau_{\text{RMS}} = 11.9$ nsec for $d = 4$ m and 12.3 nsec for $d = 8.2$ m.

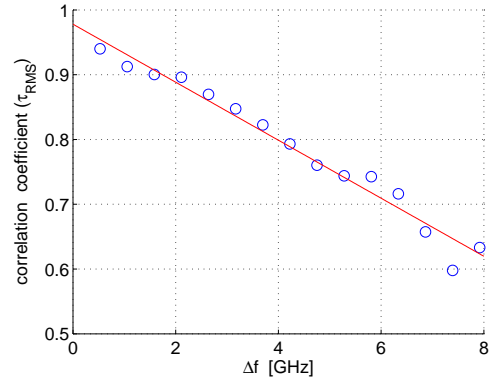


Fig. 10. RMS delay spread correlation across sub-bands, the linear fit is given by $R_{\tau_{\text{RMS}}} = -0.06\Delta f[\text{GHz}] + 0.97$.

for 100 MHz sub-band around 3.15 GHz, 5.6 GHz and 7.95 GHz for mild NLoS conditions. For extreme NLoS conditions they find RMS delay spread values of 21 nsec, 26 nsec and 43 nsec with carrier frequencies of 3.15 GHz, 5.6 GHz and 7.95 GHz. Results in [2] were calculated by thresholding the power delay profile 15 dB above the noise level, that corresponds to 45 dB from the peak in their measurements, where as our threshold was fixed by -25 dB from the temporal peak. See [12] for a demonstration of the sensitivity of the RMS delay spread to the threshold.

D. Number of Significant Taps

We count the number of channel taps that are within 10 dB of the maximal tap, and plot it vs. terminal separation in Figure 11. The number of significant taps in the full band data is an order of magnitude larger than the sub-band results, but is lower than 16 times the sub-band count. Our results are in line with [13], that show a sub-linear increase of the number of effective channel eigen-values with bandwidth. The number of significant taps calculated over adjacent sub-bands is correlated as seen in Figure 12.

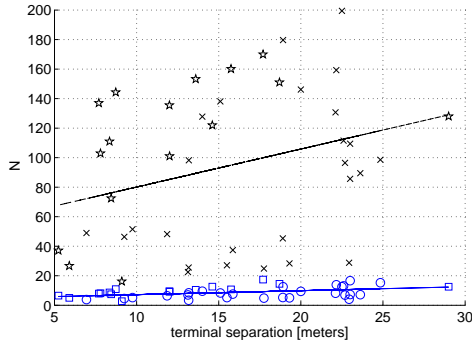


Fig. 11. The number of significant taps (within 10 dB of the maximal) vs. terminal separation, see the legend in the caption of Figure 7. The best linear fit is given by $N^{SB}(d) = 0.27 d[m] + 4.5$ (with $MSE=3.3$) and the full band fit is $N^{FB}(d) = 2.6 d[m] + 54$ (with $MSE=49.1$). Note that $16N^{SB}(d) > N^{FB}(d)$.

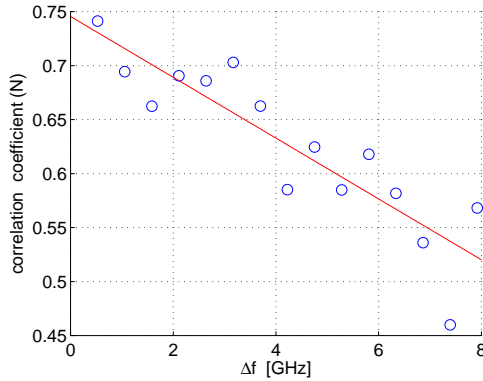


Fig. 12. Correlation of the number of significant taps across sub-bands, the linear fit is given by $R_N = -0.028\Delta f[GHz] + 0.75$.

[2] count 10 to 30 channel taps within 10 dB of the maximal for LoS and NLoS measurements with a 4.9 GHz bandwidth, it appears that a comparison with our results must take into account the dependence of the number of taps on bandwidth.

V. SUMMARY

This paper presented analysis of measured wideband indoor channel responses vs. sub-band carrier frequency with 16 bands of 528 MHz in the range 2-11 GHz. Our results show that the temporal parameters, i.e. the mean delay and RMS delay spread, as well as the number of significant channel taps, vary with antenna separation. The frequency dependence of the parameters is weak; The paper shows correlation results, that decrease approximately linearly as the frequency separation between bands increases. The paper also presents the number of significant taps and shows that the increase in the number of taps from the sub-band responses to the full-band response is not linear with the bandwidth.

The correlation of parameter values shows a clear decreasing trend as the frequency separation increases, and a very good linear fit is shown for the correlation of the mean

delays and the RMS delay spread. Note the usage of the linear fit of each parameter as the mean for the calculation of its correlation in (1). The inaccuracy of the distance-dependent linear fit raises the apparent correlation coefficient. Although our correlation results may be higher than actual correlations due to this inaccuracy of the mean, we maintain the general behavior of the results vs. frequency separation. The mean delay correlation coefficient, as well as the RMS delay spread correlation coefficient decrease to about 0.75 for bands separated by 7 GHz. The number of significant taps is correlated at about 0.55 for bands separated by 7 GHz, and the correlation is about 0.7 for neighboring bands.

ACKNOWLEDGEMENT

The authors thank Esther Solel from Elbit System for her participation in the project definition.

REFERENCES

- [1] S. S. Ghassemzadeh, L. J. Greenstain, T. Sveinsson, A. Kavčić, and V. Tarokh, "UWB delay profile models for residential and commercial indoor environments," *IEEE Transactions on Vehicular Technology*, vol. 54, no. 4, pp. 1235–1244, Jul 2005.
- [2] L. Hentilä, V. Hovinen, and M. Hämäläinen, "Sub-band analysis in UWB radio channel modeling," in *Nordic Radio Symposium/Finnish Wireless Communications Workshop (NRS/FWCW '04)*, Aug 2004, pp. 1–5.
- [3] T. Jämsä, V. Hovinen, A. Karjalainen, and J. Iinatti, "Frequency dependency of delay spread and path loss in indoor ultra-wideband channels," in *Ultra Wideband Systems, Technologies and Applications*. IEEE, Apr 2006, pp. 254–258.
- [4] J. Keignart and N. Daniele, "Subnanosecond UWB channel sounding in frequency and temporal domain," in *Ultra Wideband Systems and Technologies*. IEEE, May 2002, pp. 25–30.
- [5] I. Z. Kovács and P. C. Eggers, "Short-range UWB radio propagation investigations using small terminal antennas," in *International Workshop on Ultra Wideband Systems*, Jun 2003.
- [6] J. Kunisch and J. Pamp, "Measurement results and modeling aspects for the UWB radio channel," in *Ultra Wideband Systems and Technologies*. IEEE, May 2002, pp. 19–23.
- [7] —, "An ultra-wideband space-variant multipath indoor radio channel model," in *Ultra Wideband Systems and Technologies*. IEEE, Nov 2003, pp. 290–294.
- [8] U. Schuster and H. Bölcskei, "Ultrawideband channel modeling on the basis of information-theoretic criteria," *IEEE Transactions on Wireless Communications*, vol. 6, no. 7, pp. 2464–2475, Jul 2007.
- [9] J. Jemai, P. Eggers, G. F. Pedersen, and T. Kürner, "On the applicability of deterministic modelling to indoor UWB channels," in *The 3rd Workshop on Positioning, Navigation and Communication (WPNC)*, 2006.
- [10] J. Foerster, M. Pendergrass, and A. F. Molisch, "A channel model for ultrawideband indoor communication," Nov 2003, mitsubishi Electric Research Laboratory, Inc., TR-2003-73.
- [11] P. Pajusco and P. Pagani, "Frequency dependence of the uwb indoor propagation channel," in *The Second European Conference on Antennas and Propagation (EuCAP)*, Nov 2007, pp. 1–7.
- [12] Z. Bodnár, Z. Herczku, and I. Friges, "Noise threshold dependency of the RMS delay spread in wideband measurements of radio propagation channels," in *Telecommunications Symposium (ITS)*. SBT/IEEE, Aug 1998, pp. 312–317.
- [13] A. M. Hayar, R. Knopp, and R. Saadane, "Subspace analysis of indoor uwb channels," *EURASIP Journal on applied signal processing*, vol. 2005, no. 3, pp. 287–295, special issue on UWB - State of the art.